ZESZYTY NAUKOWE POLITECHNIKI ŁÓDZKIEJ
Nr 1108 ELEKTRYKA, z. 123 2011

KAMIL GRABOWSKI

Technical University of Łódź
Department of Microelectronics and Computer Science

PERSON IDENTIFICATION BASED ON IRIS IMAGE ANALYSIS WITH SPECIAL EMPHASIS ON HARDWARE IMPLEMENTATION – STATISTICAL ANALYSIS

Reviewer: **prof. dr hab. inż. Andrzej Napieralski**

Manuscript received: 5.07.2010

The paper presents main results of PhD dissertation concerning authentication systems based on the analysis of iris pattern. Two main threads of the work are presented: iris image segmentation and its influence on the feature extraction algorithm and methods of analysis of biometric system efficiency.

1. INTRODUCTION

Biometrics is a field of study including person identification based on their physiological or behavioral features. Among different biometric features suitable for person identification one of the most promising is a human iris due to its relatively low error rates. However, current state of the art in the iris recognition field indicates that existing methods have limited reliability when large populations are considered.

To identify a person based on his/her iris pattern, first a photo of the eye must be taken. Next, the photo is processed. In all iris recognition systems this processing consists of three major stages. Firstly, the iris region is segmented, secondly, its features are extracted. Finally the features are compared with the signatures stored previously in the database of registered users. On the basis of comparison result, the system recognizes the person standing in front of the camera.

2. IRIS SEGMENTATION

In the analysis process of biometric sample B, quality and quantity of information contained in its digital representation play a crucial role. In case of the iris biometric these factors vary along the lighting conditions and affect the whole authentication process. The absorption spectrum of melanin – the substance whose concentration makes the iris tissue colored, shows interesting characteristics for various wavelengths of light [1]. Although in current iris recognition systems near infrared light is used for illumination (due to overall ease of implementation), the meaningful increase in information content, measured as image entropy, occurs for iris images taken under visible light – figure 1. However, in this type of images correct iris segmentation is much more difficult, as it is shown in [2].

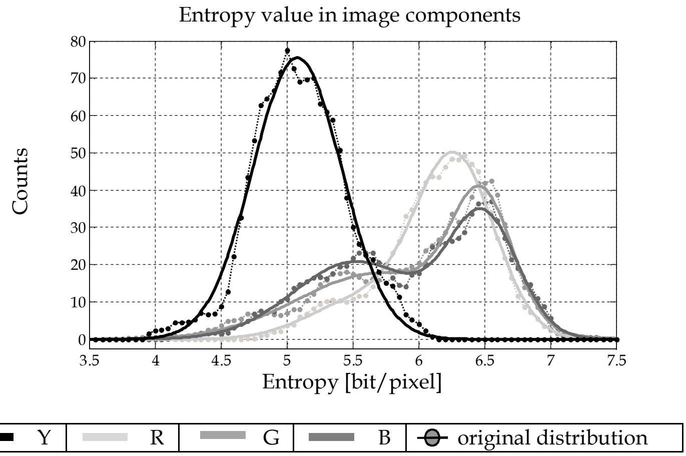

Fig. 1. Entropy distribution inside iris area obtained for two databases: ISEP (visible light in RGB components) and BATH (near infrared light in Y component)

In the iris segmentation algorithm optimized for images taken under near infrared light, a clear-cut iris-pupil boundary is used for the algorithm accuracy improvement. Similarly, the author suggested using the red (R) component of RGB iris image for segmentation algorithm optimization in images taken under visible light. Figure 2 shows the histogram of gradients recorded during the test on an iris-pupil border in each image in a group of 921 pictures taken in the visible light, contained in the ISEP database[1].

[1] *Institut Superieur d'Electronique de Paris* iris database.

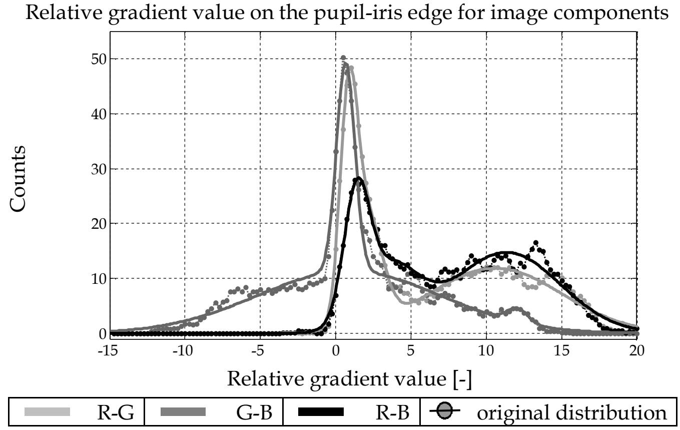

Fig. 2. Distribution of relative gradient of luminance on iris-pupil border

It may be noted that the greatest average gradient of the relative clarity of the iris-pupil boundary is observed for the red band of visible light spectrum. A small standard deviation of the distribution suggests that this feature is relatively stable for a large group of photos from the test set – table 1.

Table 1. Distribution mean values and confidence bounds comparison

	Gradient differences in image components	
	Sclera-Iris	Iris-Pupil
R-G component difference	$-0.46^{+2.32}_{-2.01}$	$6.32^{+10.07}_{-6.04}$
G-B component difference	$-0.46^{+1.67}_{-1.20}$	$1.05^{+10.87}_{-9.47}$
R-B component difference	$-1.35^{+3.76}_{-2.80}$	$7.37^{+8.76}_{-6.96}$

Therefore, a selective use of the red component on the pupil segmentation stage should result in an increased efficiency and reliability of the whole iris segmentation process for the images taken under visible light. The proposed approach was used in the software for segmentation of iris images taken in visible light, developed by W. Sankowski. The solution increased the number of correct segmentations among UBIRIS Database iris images [3] – table 2.

Table 2. Segmentation efficiency comparison [3]

Database	Segmentation efficiency	
	Grayscale	Red component
DMCS	100.00 %	100.00 %
UBIRIS (session I)	92.20 %	99.67 %

The presented results show that the selective use of the red component in the process of iris image segmentation increases the efficiency of this phase.

3. BIOMETRICAL SYSTEM EFFICIENCY

The performance of a positive biometric system is determined by error rates of false acceptance – FAR and false rejection – FRR. In general their analysis allows to compare different biometric systems and to choose the most optimal solutions depending on the assumed security strategy.

In the biometric system, the estimation of the mentioned error rates is based on the results obtained in the authentication protocol after similarity score calculation is done by the biometric comparator (1). Based on the score distributions for authentic and impostor comparisons the impact of specific factors on the authentication process can be evaluated. These can be: quality of acquisition, segmentation precision and feature extraction algorithm.

$$s = s(\hat{B}_1, \hat{B}_2) \tag{1}$$

The values of FAR and FRR are functions of the comparator threshold t (2) used to decide whether biometrics match each other. Selection of the threshold t (called also the operating point of the biometric system) depends on the assumption of safety and convenience tradeoff of the biometric system.

$$\begin{aligned} s \le t &\Rightarrow \textit{biometrics match} \\ s > t &\Rightarrow \textit{biometrics do not match} \end{aligned} \tag{2}$$

Appropriate functions FAR(t) and FRR(t) describing the error rate as a function of the threshold t can be determined by the distribution functions for the null hypothesis H_0 (biometrics match) and the alternative hypothesis H_a (biometrics do not match) (3).

$$\begin{aligned} FRR(t) &= \mathrm{P}\left(s > t \middle| H_0\right) \\ FAR(t) &= \mathrm{P}\left(s \le t \middle| H_a\right) \end{aligned} \tag{3}$$

The value of False Rejection Rate (FRR) is the probability of scores being greater than a certain threshold t, assuming that the null hypothesis H_0 is true. Accordingly, the value of False Acceptance Rate is the probability of scores being less than a certain threshold t, assuming that the alternative hypothesis H_a is true. In both cases it is assumed that a low scoring value calculated by the biometric comparator is equivalent to strong evidence that the compared biometrics are conformable.

Recognized criteria for assessing the interaction between error rates FAR and FRR, defined for any value of the decision threshold *t*, are Receiver Operating Characteristics, called also ROC curves (4) [4].

$$ROC(t) = (FAR(t), FRR(t)) \tag{4}$$

The obtained estimates of FAR and FRR curves cannot yet definitively decide about the general performance of a biometric system. Keeping in mind that the data source is a random process, one would know certainty of the obtained results for a given *t*. For this purpose, an additional element of statistical analysis of biometric data is the estimation of confidence bounds for FAR and FRR curves. In other words it is necessary to find intervals of true average error rate values for false rejection and false acceptance functions, on a certain confidence level (1-α) for many possible decision threshold values *t* (5).

$$\begin{aligned} E_{FRR}(t) &\in \left(\overline{FRR}(t) - \Delta FRR_1(t,\alpha),\ \overline{FRR}(t) + \Delta FRR_2(t,\alpha)\right) \\ E_{FAR}(t) &\in \left(\overline{FAR}(t) - \Delta FAR_1(t,\alpha),\ \overline{FAR}(t) + \Delta FAR_2(t,\alpha)\right) \end{aligned} \tag{5}$$

In this particular case the best solution for such estimation is to use the bootstrap method proposed by Efron modified by the author [5].

The main aim of the mentioned analysis was the investigation of segmentation algorithm accuracy influence on the final authentication result. The precision of the algorithm is graded as follows:

- pupil segmentation by b-spline curve and iris outer boundary segmentation by ellipse with occlusions masking – Precise variant;
- pupil and iris outer boundary segmentation by non-concentric circles with occlusions masking – Simple variant;
- pupil segmentation by circle and iris outer boundary segmentation by ellipse with occlusions masking – mixed variant 1 (CircleEllipse);
- pupil segmentation by b-spline curve and iris outer boundary segmentation by circle with occlusions masking – mixed variant 2 (SplineCircle).

The source for scoring are comparisons among images contained in two databases: ISEP (images in visible light) and BATH (images in the near-infrared light).

On the basis of preliminary observations of ROC curves, due to the large confidence intervals at 90% level, it was difficult to identify the ultimate impact of segmentation accuracy to the performance of the biometric system. Therefore, for each individual comparison an additional differential scoring was calculated in order to detect changes in score value caused by accuracy increase of the segmentation algorithm. As a reference, scores generated for a simple segmentation variant were assumed (6).

$$\Delta s_{Simple-\{Precise,SplineCircle,CircleEllipse\}} = s_{Simple} - s_{\{Precise,SplineCircle,CircleEllipse\}} \quad for\ H_0$$
$$\Delta s_{Simple-\{Precise,SplineCircle,CircleEllipse\}} = s_{\{Precise,SplineCircle,CircleEllipse\}} - s_{Simple} \quad for\ H_a \qquad (6)$$

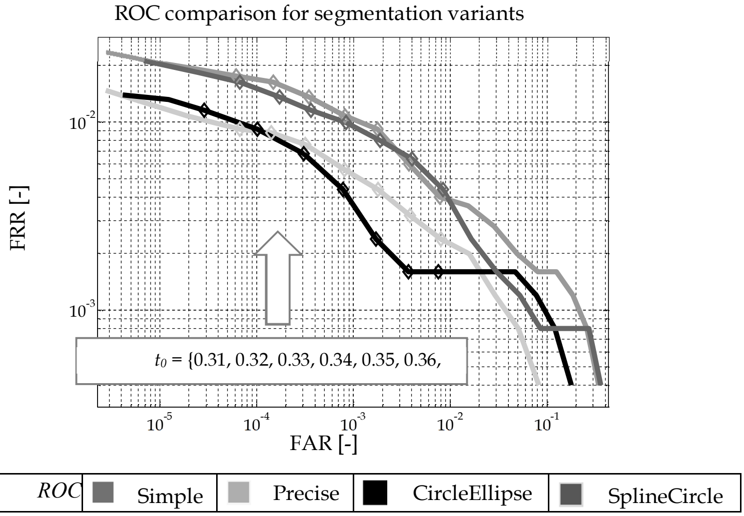

Fig. 3. ROC Curves for four variants of segmentation algorithm applied in ISEP database. Selected operating points are indicated

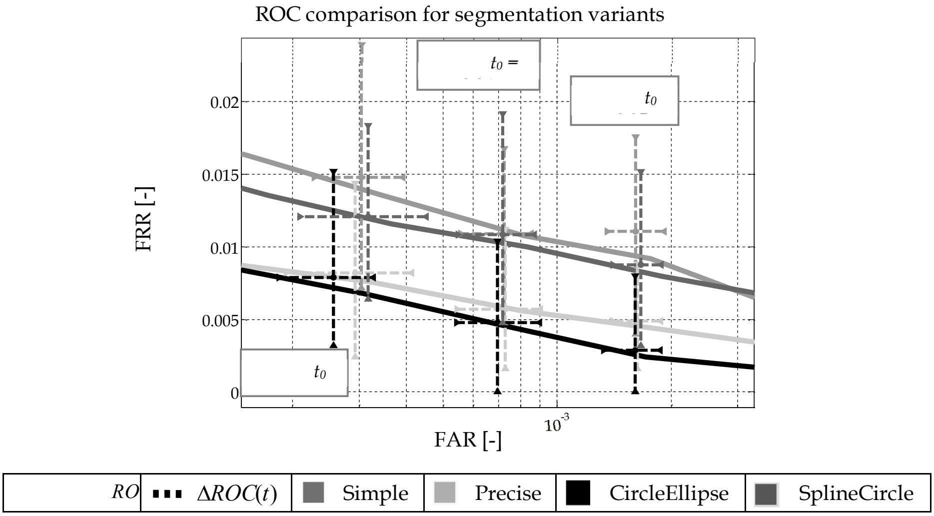

Fig. 4. ROC curves fragments for four variants of segmentation algorithm applied in ISEP. Confidence bounds at 90% level are indicated for selected operating points of the system

An example of the relative scores presented in figure 5, shows almost normal distributions. The average values of these distributions are positive, but very close to zero. For the ISEP database a slight predominance of comparisons, where an increase of the segmentation precision results in a reduction in the scoring for H_0 hypothesis, is present. Furthermore, for the alternative hypothesis H_a the dominance of comparisons, where an increase of the segmentation precision results in a deterioration of the results, is obtained (shifting the distribution toward smaller score values).

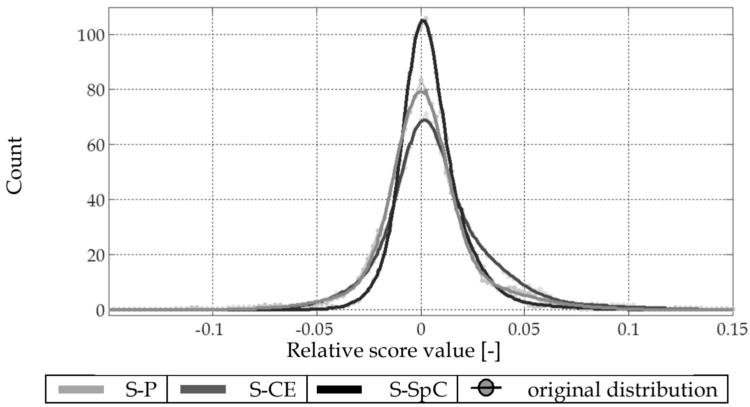

Fig. 5. Relative score distribution for the chosen segmentation variants for null hypothesis and ISEP database

It should be noted that in each of these cases, the distribution of the relative score values extends to both positive and negative, which means almost equal number of improvements and deteriorations in identification as a result of the segmentation accuracy increase.

Table 3. Comparison of the distributions parameters of the relative scores for ISEP database (for a confidence level at 95%)

	Mean relative score value (ISEP database)	
	$s\|H_0$ comparisons	$s\|H_a$ comparisons
$\Delta s_{Simple\text{-}Precise}$	$\left(8.8\cdot10^{-3}\right)^{+69.9}_{-48.7}$	$\left(-1.0\cdot10^{-3}\right)^{+59.5}_{-60.9}$
$\Delta s_{Simple\text{-}CircleEllipse}$	$\left(4.2\cdot10^{-3}\right)^{+60.0}_{-42.2}$	$\left(0.8\cdot10^{-3}\right)^{+54.1}_{-55.4}$
$\Delta s_{Simple\text{-}SplineCircle}$	$\left(4.7\cdot10^{-3}\right)^{+37.6}_{-27.1}$	$\left(-1.8\cdot10^{-3}\right)^{+41.0}_{-41.3}$

4. CONCLUSIONS

All stages of the iris image processing are the possible sources of errors resulting in an incorrect person identification. Firstly, the analysis related to true reasons of the above mentioned errors was done. Several improvements were proposed to help typical iris recognition systems become more reliable. The above analysis leads to the conclusion that increasing the segmentation accuracy by applying a precise modeling of iris borders curves, does not cause a significant increase in the number of comparisons for which the authentication process result gives additional evidence to support any of the hypotheses. Wide confidence intervals of the FAR and FRR estimates show a large dispersion in biometric scoring, which means that the feature extraction methods based on a texture analysis are not very stable in the sense of the results of authentication.

REFERENCES

[1] **Wistrand P., Stjernschantz J., Olsson K.:** The incidence and time-course of latanoprost-induced iridial pigmentation as a function of eye color, *Survey of Ophthalmology* 41(S2), 1997, pp. S129-S138.
[2] **Sankowski W.:** Algorytmy segmentacji obrazu oka, dla potrzeb systemu identyfikacji osób w oparciu o wzór tęczówki, *Rozprawa doktorska,* Politechnika Łódzka, 2009.
[3] **Sankowski W., Grabowski K., Napieralska M., Zubert M.:** Eyelids Localization Method Designed for Iris Recognition System, Proceedings of the 14th International Conference of Integrated Circuit and Systems (MIXDES '07), Ciechocinek, Poland 21-23 June 2007, pp. 622-627.
[4] **Bolle R. M., Connel J. H., Pankanti S., Ratha N. K., Senior A. W.:** Guide to Biometrics, Springer Science&Buisness Media Inc., New York NY, USA, 2004Omega. The temperature Handbook 2000. Vol. 29.
[5] **Grabowski K.:** Analiza wydajności systemów biometrycznych na przykładzie baz tęczówek ISEP oraz BATH, Raport wewnętrzny, Politechnika Łódzka, 2009.

IDENTYFIKACJA OSÓB NA PODSTAWIE ANALIZY OBRAZU TĘCZÓWKI OKA ZE SZCZEGÓLNYM UWZGLĘDNIENIEM MOŻLIWOŚCI IMPLEMENTACJI SPRZĘTOWEJ

Streszczenie

W artykule przedstawiono główne rezultaty badań zawartych w rozprawie autora dotyczącej systemów uwierzytelniania osób na podstawie obrazu tęczówki

oka. Zaprezentowano dwa główne wątki pracy doktorskiej: segmentacji obrazu tęczówki i jej wpływu na proces ekstrakcji cech oraz metod analizy wydajności biometrycznej systemów uwierzytelniania.

Promotor prof. dr hab. Andrzej Napieralski
Recenzenci pracy doktorskiej:

1. prof. dr hab. inż. Kazimierz Wiatr, AGH
2. dr hab. inż. Krzysztof Ślot, prof. PŁ